Raman-active phonons of a twin-free $YBa_2Cu_3O_7$ crystal: A complete polarization analysis

K. F. McCarty
Sandia National Laboratories, Livermore, California 94551

J. Z. Liu and R. N. Shelton
Department of Physics, University of California-Davis, Davis, California 95616

H. B. Radousky
Lawrence Livermore National Laboratory, Livermore, California 94550

(Received 13 November 1989)

A complete Raman analysis has been performed on a high-quality $YBa_2Cu_3O_7$ crystal made free of twins by a mechanical detwinning process. Marked *a-b* anisotropy is observed in the intensity of the A_g phonons at 116, 335, and 495 cm^{-1}. At room temperature, the α_{yy} component of the polarizability tensor of the 116-cm^{-1} phonon is strongly coupled to an electronic continuum, the α_{xx} component is less strongly coupled, and the coupling of the α_{zz} component is not apparent in the Raman line shape. B_{2g} and B_{3g} phonon pairs are reproducibly found at 70 and 83 cm^{-1}, 142 and 140 cm^{-1}, 210 and 303 cm^{-1}, and 579 and 526 cm^{-1}. Comparison of the observed B_{2g}-B_{3g} pairs to literature calculations of frequencies is made.

INTRODUCTION

The high-temperature superconductor $YBa_2Cu_3O_7$ has been studied extensively by Raman spectroscopy.[1] The majority of investigations have analyzed "single" crystals containing high densities of twins that interchange the *a* and *b* directions in the crystals. On any macroscopic scale, the twins make the *a* and *b* directions indistinguishable. This is unfortunate, however, since the *a* and *b* directions are markedly different in the orthorhombic structure of $YBa_2Cu_3O_7$.[2] As seen in Fig. 1, along the $b=y$ direction are the O(1) atoms that form the Cu(1)-O(1) "chains." There are no equivalent oxygen atoms along the $a=x$ direction and hence no Cu(1)-O(1) chains in this direction. Because of this *a-b* anisotropy, a complete analysis of the Raman-active phonons is not possible using twinned crystals. In particular, assignment of the B_{2g} and B_{3g} modes cannot be made by studying twinned crystals. The eigenvectors of the B_{2g} and B_{3g} modes are essentially the same; the B_{2g} modes involve atomic motion along the *a* axis and the B_{3g} modes involve motion along the *b* axis.[3]

Several Raman studies of twin-free $YBa_2Cu_3O_7$ crystals have been reported.[4-6] These measurements revealed differences in the relative intensities of the A_g phonons depending upon whether the polarization of the incident and scattered light was along the direction of the Cu(1)-O(1) chains (i.e., the *b* direction) or perpendicular to the direction of the Cu(1)-O(1) chains (i.e., the *a* direction). Measurements below T_c revealed differences in the electronic Raman scattering depending upon the orientation of the polarization with respect to the Cu(1)-O(1) chains.[5] Unfortunately, the existing studies either do not provide an analysis of all crystal orientations or do not extend sufficiently low in frequency to see all of the Raman-active vibrations.

Here we report a complete polarization analysis of the Raman-active phonons of a true single crystal of $YBa_2Cu_3O_7$, that is, a twin-free crystal produced by a mechanical detwinning process. New and important features are found and the results of previous, less complete investigations are largely confirmed. At room tem-

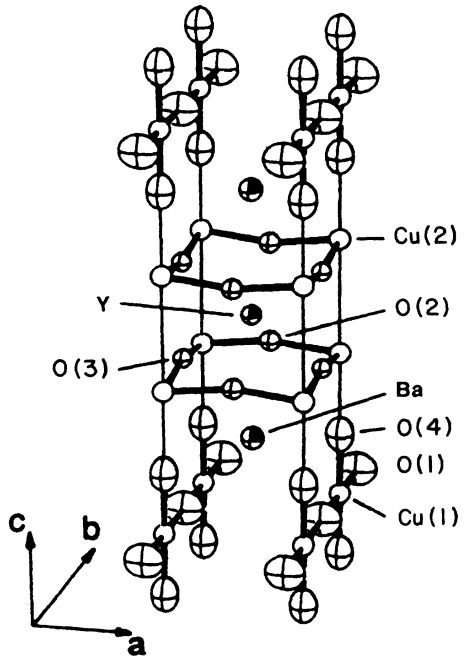

FIG. 1. Illustration of orthorhombic $YBa_2Cu_3O_7$ showing the convention used to distinguish the atoms of the unit cell. The Cu(1)-O(1) "chains" run along the *b* direction. Adapted from Jorgensen *et al.* (Ref. 2).

perature, the degree of electron-phonon coupling of the vibration of Ba along the c axis varies greatly with polarization geometry. For polarization within the Cu(2)-O(2) and (3) planes and parallel to the Cu(1)-O(1) chains, the 116-cm^{-1} mode is strongly coupled to an electronic continuum. For polarization within the Cu(2)-O(2) and (3) planes and perpendicular to the Cu(1)-O(1) chains, the mode is less strongly coupled to the electronic continuum. For polarization perpendicular to the Cu(2)-O(2) and (3) planes, the coupling is not apparent in the Raman line shape. Pairs of B_{2g} and B_{3g} phonons are reproducibly found at 70 and 83 cm^{-1}, 142 and 140 cm^{-1}, 210 and 303 cm^{-1}, and 579 and 526 cm^{-1}. Comparison of the observed B_{2g}-B_{2g} pairs to literature calculations[3,7] of frequency is made.

EXPERIMENT

A twin-free crystal of $YBa_2Cu_3O_7$ was produced by a mechanical detwinning process described, along with the crystal-growth process, in detail elsewhere.[8] The orientation of the a and b directions in the crystal was uniquely determined by the detwinning procedure. The crystal was annealed in flowing O_2 for about 120 h at 400 °C in order to ensure that the stoichiometry was as close as possible to O_7. The crystal was a nearly square platelet about $300\times300\times70$ μm^3 in dimension. The a and b crystallographic directions were along the edges of the platelet.

Figure 2 shows the magnetization analysis of the twin-free crystal of $YBa_2Cu_3O_7$ obtained using a SQUID magnetometer. The crystal was mounted with the c axis approximately perpendicular to the applied field. The small size of the sample (about 40 μg) required the application of a field of 20 Oe to obtain reasonably noise-free data.

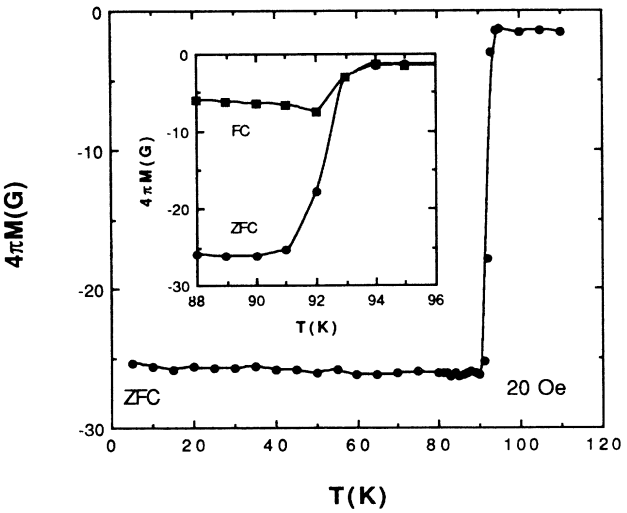

FIG. 2. Magnetization analysis of twin-free $YBa_2Cu_3O_7$ crystal for both zero-field cooling (ZFC) and field cooling (FC) in an applied magnetic field of 20 Oe. The superconducting transition is extremely sharp, beginning at 93 K, with a 10–90 % transition width of 1.6 K.

The superconducting transition was very sharp, with a 10–90 % transition width of 1.6 K. The onset of the diamagnetic transition was observed to begin at 93 K, which is consistent with the sample having an oxygen stoichiometry very near to 7.0. The ratio of the field-cooled (FC) magnetization to the zero-field-cooled (ZFC) magnetization was found to be 25%, which is consistent with a fully superconducting sample measured in applied field of 20 Oe. The apparent Meissner fraction is reduced due to flux-creep effects, and serves only as a lower bound on the fraction of the material that is superconducting.[9] Larger crystals from the same batch measured at 5 Oe gave Meissner fractions of 60%.[8]

All Raman measurements were made at room temperature using a microprobe apparatus that has been previously described.[10] A 40× objective lens with a numerical aperture of 0.6 produced a laser spot of about 1 μm in diameter. Incident power of the 488-nm laser was 0.4 mW. Data accumulation times varied between 10 min and 3 h depending upon the strength of the Raman signal. In order to reduce the collection of elastically scattered radiation, a 180° backscattering geometry was utilized in which the surface normal of the crystal was rotated ~20° from the direction of the incident laser beam. For the B_{2g} and B_{3g} polarization geometries (see Fig. 5), argon gas was flowed over the crystal to eliminate interference from the rotational Raman lines of atmospheric gases (O_2 and N_2).

RESULTS AND DISCUSSION: A_g MODES

At the center of the Brillouin zone of $YBa_2Cu_3O_7$, there are fifteen Raman-active vibrational modes; five of A_g symmetry, five of B_{2g} symmetry, and five of B_{3g} symmetry. Figures 3 and 4 illustrate Raman spectra of the twin-free crystal of $YBa_2Cu_3O_7$ obtained with polarization geometries permitting A_g vibrational modes. The A_g modes, observed at 116, 149, 335, 435, and 495 cm^{-1}, are well studied.[1] For completeness, the frequencies observed for the A_g modes in all of the polarization geometries are listed in Table I, along with the results of lattice-dynamic calculations.[7] The mode at 335 cm^{-1} has B_{1g} symmetry in tetragonal $YBa_2Cu_3O_{7-x}$. Since $\alpha_{xx}\approx-\alpha_{yy}$ for the 335-cm^{-1} mode, while $\alpha_{xx}\approx\alpha_{yy}$ for the other A_g modes,[3] the 335-cm^{-1} mode has a different polarization dependence than the other A_g modes in orthorhombic $YBa_2Cu_3O_{7-x}$.

As previously observed,[4,5] the a-b anisotropy is apparent in the spectra of Fig. 3, obtained with the incident laser beam propagating along the c axis. The relative intensity of the 116- and 495-cm^{-1} phonons is greater when the polarization of the incident and scattered light is along the Cu(1)-O(1) chains (spectrum second from the top) than when the polarization of the incident and scattered light is perpendicular to the Cu(1)-O(1) chains (top spectrum of Fig. 3). The Ba vibration at 116 cm^{-1} has been observed to have an asymmetric line shape caused by the interference of the scattering of the discrete phonon with the scattering of an electronic continuum.[5] The interference is constructive on the high-frequency side of the phonon and destructive on the low-frequency side.

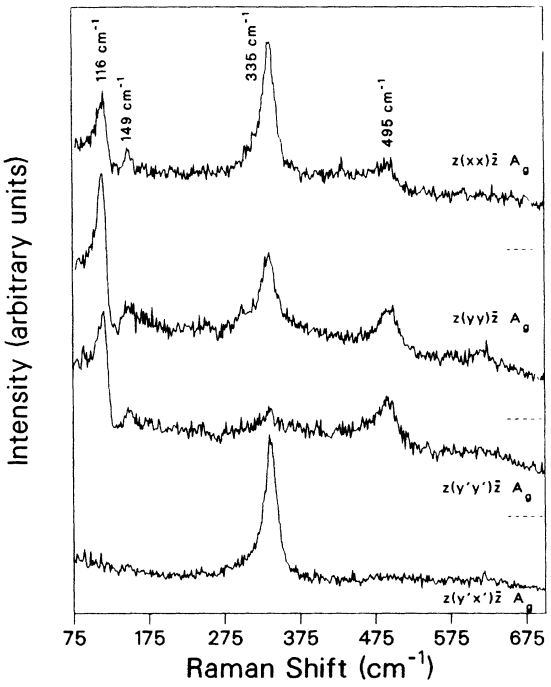

FIG. 3. Raman spectra of twin-free $YBa_2Cu_3O_7$ obtained with the incident laser beam propagating perpendicular to the Cu(2)-O(2) and (3) planes, i.e., along the $z=c$ axis. In the Porto notation, y refers to polarization along the b axis of the crystal, y' refers to polarization at 45° to the a and b axis, and x' refers to polarization at 90° to y'. Baseline for the bottom spectrum is the x axis; baselines for the upper three spectra are the horizontal, dashed lines.

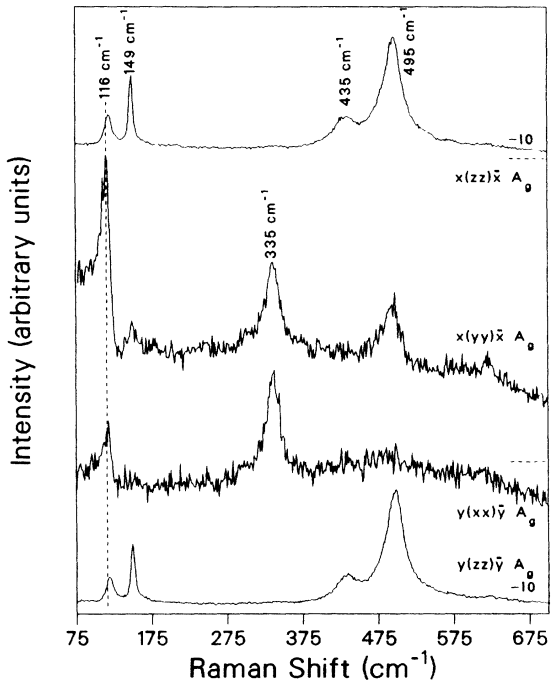

FIG. 4. Raman spectra of twin-free $YBa_2Cu_3O_7$ obtained with the incident laser beam propagating parallel to the Cu(2)-O(2) and (3) planes. Note scale factor applied to $y(zz)\bar{y}$ and $x(zz)\bar{x}$ spectra. Baseline of the bottom two spectra is the $x=a$ axis; baselines of the upper two spectra are the horizontal, dashed lines. For the (zz) spectra, there is no evidence of antiresonant behavior of the 116-cm^{-1} mode.

The destructive interference causes the intensity to "dip" below the baseline on the high-frequency side. Here, this "antiresonant" behavior of the 116-cm^{-1} phonon is pronounced with the polarization of the incident and scattered light along the Cu(1)-O(1) chains (spectrum second from the top) and with the polarization of the incident and scattered light at 45° to the direction to the Cu(1)-O(1) chains (spectrum third from the top). In contrast, less antiresonant behavior is observed when the polarization of the incident and scattered light is perpendicular to the Cu(1)-O(1) chains (top spectrum of Fig. 3). That is, in this spectrum neither the constructive interference on the

TABLE I. Raman shifts for twin-free $YBa_2Cu_3O_7$ crystal.

			Experimental					
$z(xx)\bar{z}$ [a]	A_g [b]	α_{xx} [c]	116[d]	149	336		493	
$z(yy)\bar{z}$	A_g	α_{yy}	114	149	335		495	617[e]
$z(y'y')\bar{z}$	A_g	$\alpha_{xx}+\alpha_{yy}$	116	149	335		493	
$z(y'x')\bar{z}$	A_g	$-\alpha_{xx}+\alpha_{yy}$			335			
$x(zz)\bar{x}$	A_g	α_{zz}	119	149		435	497	
$x(yy)\bar{x}$	A_g	α_{yy}	115		336		495	621[e]
$y(xx)\bar{y}$	A_g	α_{xx}	119		336			
$y(zz)\bar{y}$	A_g	α_{zz}	119	149		435	498	
			Calculated[f]					
	A_g		116	157	355	378	508	

[a]Polarization geometry in Porto notation.
[b]Symmetry of phonon permitted by polarization geometry.
[c]Component of polarizability tensor permitted by polarization geometry.
[d]All values in cm^{-1}.
[e]Mode observed in addition to the permitted A_g modes.
[f]Reference 7.

low-frequency side nor the destructive interference on the high-frequency side are as pronounced as in the $z(yy)\bar{z}$ spectrum.

Previously unreported features are seen in the spectra of Fig. 4, obtained with the incident laser beam propagating along the Cu(2)-O(2) and (3) planes. The intensities of the 116 and 495 cm^{-1} phonons are greater when the polarization is along the direction of the Cu(1)-O(1) chains (spectrum second from the top) than when the polarization is perpendicular to the Cu(1)-O(1) chains (spectrum third from the top). Further, the degree of antiresonance of the 116-cm^{-1} phonon is much greater for polarization along the Cu(1)-O(1) chains than for polarization perpendicular to the Cu(1)-O(1) chains (spectrum third from the top). The results of Fig. 4 are an independent verification of those of Fig. 3 since both sets of polarization geometries measure either the α_{xx} or α_{yy} component of the polarizability tensor.

As seen in the bottom and top spectra of Fig. 4, the two spectra obtained with zz polarization (i.e., with incident and scattered polarization along the c axis) are virtually identical. This is expected since the anisotropy introduced by the Cu(1)-O(1) chains is not seen by zz polarization. Importantly, there is no apparent antiresonance of the Ba vibration in this geometry. That is, for zz polarization, the peak is highly symmetric with no indication of destructive interference on the high-frequency side. The lack of interference also results in a maximum peak intensity at 119 cm^{-1} for the $x(zz)\bar{x}$ and $y(zz)\bar{y}$ spectra versus 115 cm^{-1} for the $x(yy)\bar{x}$ spectrum. The lack of antiresonant behavior for zz polarization is not due to the lack of an electronic continuum with which to interfere. Indeed, spectra with zz polarization had intense, flat "backgrounds" resulting from electronic scattering extending from at least 75 to 700 cm^{-1}. This background is about twice as intense as the background of the $z(xx)\bar{z}$ and $z(yy)\bar{z}$ spectra of Fig. 3.

The results of Fig. 4 have several interesting implications. First, the analysis was performed at the "edges" of the platelet and showed marked a-b anisotropy. This establishes that the crystal was successfully detwinned throughout, not just in the center. Significantly, no antiresonant behavior is observed for the Ba vibration (116 cm^{-1}) in the spectra with zz polarization despite intense scattering from an electronic continuum. Taken together with the results of Fig. 3, this indicates that the α_{yy} component of the polarizability tensor of the 116-cm^{-1} phonon is strongly coupled to the electronic continuum, the α_{xx} component is less strongly coupled, and the coupling of the α_{zz} component is not manifest in the Raman line shape.

RESULTS AND DISCUSSION: B_{2g} and B_{3g} MODES

Figure 5 illustrates spectra obtained in polarization geometries that permit $B_{2g}(y(zx)\bar{y})$ and $B_{3g}(x(zy)\bar{x})$ vibrational modes. The scattering intensity in these geometries is extremely weak, well over 100 times less intense than that observed in the $y(zz)\bar{y}$ geometry, for example. Except for the mode at 335 cm^{-1}, the A_g modes are shown for comparison in the bottom spectrum of Fig. 5, obtained with $y(zz)\bar{y}$ geometry. Comparison of the spectra shows that all of the A_g modes can be observed in the B_{2g} and B_{3g} geometries, a result of imperfect polarization, i.e., "polarization leakage." However, additional peaks are present in the B_{2g} and B_{3g} geometries that are not the A_g modes. It is emphasized that these peaks, while extremely weak, were reproducibly observed from different areas of the crystal. Also, the peaks are not instrumental artifacts. By changing the rotation of the grating in the spectrograph, different frequency ranges were dispersed on the detector and the peaks were reproduced at constant values of Raman shift. This eliminates the possibility of artifacts produced by nonuniform response of the multichannel detector or stray light. Further, these peaks are believed to be intrinsic features of $YBa_2Cu_3O_7$; spectra were collected from regions that were very mirrorlike in appearance. Finally, the peaks exhibit the well-behaved polarization dependence expected of B_{2g} and B_{3g} phonons. This dependence could be exhibited only by a "pathological" impurity that is epitaxial with the $YBa_2Cu_3O_7$ crystal, an unlikely possibility.

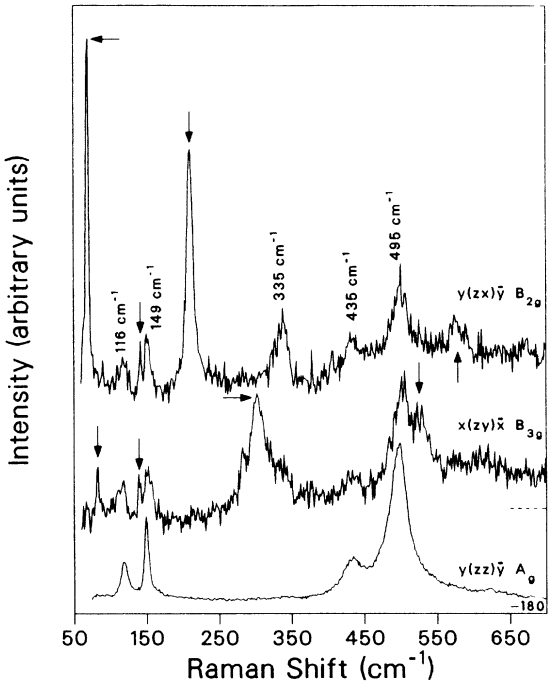

FIG. 5. Raman spectra of twin-free $YBa_2Cu_3O_7$ in polarization geometries allowing B_{2g} (top spectrum) and B_{3g} (middle spectrum) modes. Peaks marked with arrows were reproducibly observed and are B_{2g} and B_{3g} modes. The five A_g modes are labeled with frequencies and appear as a result of polarization leakage, as seen by comparison with the bottom spectrum that shows all the A_g modes except the 335-cm^{-1} mode. Baseline for the bottom two spectra is the x axis; baseline for the upper spectrum is the horizontal, dashed line. Note scale factor applied to the $y(zz)\bar{y}$ spectrum.

Table II gives the frequencies of the observed B_{2g} and B_{3g} modes along with the results from calculations of the

TABLE II. B_{2g} and B_{3g} Raman modes of twin-free $YBa_2Cu_3O_7$ crystal.

		Experimental					
$y(zx)\bar{y}$ [a]	B_{2g} [b]	α_{zx} [c]	70[d]	142	210	e	579
$x(zy)\bar{x}$	B_{3g}	α_{zy}	83	140	303	e	526
		Calculated[f]					
B_{2g}			73	142	356	429	564
B_{2g}			92	137	412	496	544

[a]Polarization geometry in Porto notation.
[b]Symmetry of phonon permitted by polarization geometry.
[c]Component of polarizability tensor permitted by polarization geometry.
[d]All values in cm^{-1}.
[e]Allowed mode not observed.
[f]Reference 7.

lattice dynamics.[7] The B_{2g} geometry contains peaks at 70, 142, 210, and 579 cm^{-1}, while the B_{3g} spectrum exhibits peaks at 83, 140, 303, and 526 cm^{-1}. The B_{2g} and B_{3g} modes are essentially the same vibrations with the B_{2g} modes involving atomic motion along the a axis and the B_{3g} modes involving motion along the b axis.[3] However, due to the Cu(1)-O(1) chains that run along the b direction, the B_{2g} and B_{3g} modes can differ in frequency, particularly for modes involving atoms adjacent to the Cu(1)-O(1) chains, i.e., the Y and O(4) atoms. Assignment of two of the observed B_{2g} modes and their corresponding B_{3g} modes is straightforward. The peaks at 70 cm^{-1} (B_{2g}) and 83 cm^{-1} (B_{3g}) involve motion primarily Ba and according to calculations of the lattice dynamics;[7] these modes are estimated to be at 73 cm^{-1} and 92 cm^{-1}, respectively. The peaks at 142 cm^{-1} (B_{2g}) and 140 cm^{-1} (B_{3g}) involve motion primarily of Cu(2), the Cu atoms of the Cu(2)-O(2) and (3) planes. According to calculations of the lattice dynamics,[7] these modes are estimated to be at 142 cm^{-1} and 137 cm^{-1}, respectively.

The next B_{2g}-B_{3g} pair is found at 210 and 303 cm^{-1}. These peaks have also been observed by Gasparov *et al.*,[6] and like them, we assign these peaks to vibration of O(4), the O atoms that "bridge" the Cu(2)-O(2) and (3) planes and the Cu(1)-O(1) chains. The agreement between experiment and calculation in absolute frequency is poor; the B_{2g} and B_{3g} modes of O(4) vibration are calculated to be at 356 and 412 cm^{-1}, respectively. One aspect of the comparison is encouraging, however. The calculated a-b anisotropy is very large,[7] specifically, 56 cm^{-1}, and the observed anisotropy is also very large, specifically, 93 cm^{-1}.

While there are two additional B_{2g}-B_{3g} pairs that are allowed, only one B_{2g} (579 cm^{-1}) and one B_{3g} (526 cm^{-1}) mode have been experimentally observed. Burns *et al.*[11] have also observed a peak at 585 cm^{-1} in a zy polarization geometry. Both of the remaining, allowed B_{2g}-B_{3g} pairs involve vibration of O(2) and O(3), the O atoms of the Cu(2)-O(2) and (3) planes.[3] Lattice-dynamic calculations[7] indicate that the in-phase vibrations of O(2) and O(3) are at lower frequencies than the out-of-phase vibrations, with the lowest frequency vibration being at 429 cm^{-1} and the highest frequency vibration being at 564 cm^{-1}. In Table II, the observed vibrations at 579 and 526 cm^{-1} have been assigned to the out-of-phase vibration of O(2) and O(3). It is cautioned that this assignment is not definitive, and that the definitive assignment cannot be made until the remaining B_{2g} and B_{3g} modes are experimentally identified. These unobserved modes are either weak, broad, or masked by leakage of the A_g modes.

Several comments are in order concerning the results of previous investigations. Gasparov *et al.*[6] report observation of both B_{2g} and B_{3g} modes at 340 cm^{-1}. This assignment is very difficult to support given the A_g mode at 335 cm^{-1} and its inevitable appearance through polarization leakage (see Fig. 5). Some investigations have concluded that modes at 220 and 580 cm^{-1} result from vibrational modes that are not formally Raman active but derive intensity from the presence of symmetry-breaking oxygen vacancies.[1] Several observations support the assignment that the peaks observed here at 210 and 579 cm^{-1} are indeed allowed B_{2g} vibrations. First and foremost, the 210 and 579 cm^{-1} peaks have their greatest relative intensity in the polarization geometry permitting B_{2g} modes. Second, the present crystal contains few oxygen vacancies, as evidenced by the extremely sharp diamagnetic transition at 93 K. Third, when peaks near 220 and 580 cm^{-1} have been observed by others and ascribed to defect-induced scattering, the peaks have been observed with the incident and scattered light propagating along the c axis. For this polarization geometry (see Fig. 3), no peaks near 220 and 580 cm^{-1} are apparent in spectra of the present crystal.

Finally, it is suggested that while there can be a defect-induced peak near 580 cm^{-1}, this peak is distinct from the mode at 579 cm^{-1} identified here as B_{2g} in symmetry. Measurements at elevated temperatures, where the density of oxygen vacancies is great, reveal that the largest tensor component of the 580 cm^{-1} peak is α_{zz}.[10] There is no obvious peak near 580 cm^{-1} for either the $x(zz)\bar{x}$ or the $y(zz)\bar{y}$ spectra (see Fig. 4), the polarization geometries for which the defect-induced mode is most dominant. The lack of observation of the defect-induced mode in its dominant polarization geometry establishes that scattering from this mode is absent in the present crystal. Therefore, a distinct mode accounts for the 579-cm^{-1} peak of B_{2g} symmetry observed here.

Concerning the assignment of the defect-induced mode at 580 cm^{-1}, the strong α_{zz} component suggests that the vibration is dominated by vibration along the c axis. The most likely candidate is the ir-active, B_{1u} mode calculated to occur at $\sim$575 cm^{-1}.[7] The eigenvector of this mode involves vibration of O(4), O(1), and Cu(1) along the c axis.[3] A similar conclusion has been reached by Poberaj *et al.*[12] Following the reasoning of Thomsen *et al.*,[4] the intensity of the B_{1u} mode should be greatest for polarization along the Cu(1)-O(1) chains, as observed.[4]

SUMMARY

A complete Raman analysis has been performed of a twin-free crystal of $YBa_2Cu_3O_7$ with an extremely sharp

superconducting transition beginning at 93 K. While strong electronic scattering is observed for all polarization geometries except B_{2g} and B_{3g}, strong coupling of this continuum to the 116-cm^{-1} phonon is only observed for the α_{yy} component. This observation should help clarify the origin of the electronic states that are coupled to the Ba vibration.

Several B_{2g} and B_{3g} modes have been conclusively identified for the first time. The observed frequencies of the two B_{2g}-B_{3g} pairs lowest in frequency agree very well with calculations.[7] The agreement for the vibration of O(4) is poor, although the experimentally observed *a-b* anisotropy is large, in agreement with calculations.[7] The observation of the B_{2g} and B_{3g} modes now allows the measurement of their temperature dependence. The modes at 142 and 140 cm^{-1} are dominated by Cu(2) motion in the Cu(2)-O(2) and (3) planes. The modes at 526 and 579 cm^{-1} are dominated by O(2) and O(3) motion in the Cu(2)-O(2) and (3) planes. The temperature dependence of these modes is particularly important since they involve vibration of the Cu and O atoms of the Cu(2)-O(2) and (3) planes, the structural element that carries the supercurrent.

ACKNOWLEDGMENTS

Work at Sandia National Laboratories was supported by the U.S. Department of Energy, Office of Basic Energy Sciences, Division of Materials Sciences under Contract No. DEAC04-76DP00789. Work at Lawrence Livermore National Laboratory and University of California-Davis was performed under the auspices of the U.S. Department of Energy under Contract No. W-7405-ENG-48.

[1]See, for example, the following review articles: J. R. Ferraro and V. A. Maroni, Appl. Spect. (to be published); R. Feile, Physica C **159**, 1 (1989).

[2]J. D. Jorgensen, M. A. Beno, D. G. Hinks, L. Soderholm, K. J. Volin, R. L. Hitterman, J. D. Grace, I. K. Schuller, C. U. Segre, K. Zhang, and M. S. Kleefisch, Phys. Rev. B **36**, 3608 (1987).

[3]R. Liu, C. Thomsen, W. Kress, M. Cardona, B. Gegenheimer, F. W. de Wette, J. Prade, A. D. Kulkarni, and U. Schröder, Phys. Rev. B **37**, 7971 (1988).

[4]C. Thomsen, M. Cardona, B. Gegenheimer, R. Liu, and A. Simon, Phys. Rev. B **37**, 9860 (1988).

[5]F. Slakey, S. L. Cooper, M. V. Klein, J. P. Rice, and D. M. Ginsberg, Phys. Rev. B **39**, 2781 (1989).

[6]L. V. Gasparov, V. D. Kulakovskii. O. V. Misochko, and V. B. Timofeev, Physica C **157**, 341 (1989).

[7]W. Kress, U. Schröder, J. Prade, A. D. Kulkarni, and F. W. de Wette, Phys. Rev. B **39**, 2906 (1988).

[8]J. Z. Liu, M. D. Lan, P. Klavins, and R. N. Shelton, Phys. Lett. (to be published).

[9]Y. Yeshurun and A. P. Malozemoff, Phys. Rev. Lett. **60**, 2202 (1988).

[10]K. F. McCarty, J. C. Hamilton, R. N. Shelton, and D. S. Ginley, Phys. Rev. B **38**, 2914 (1988).

[11]G. Burns, F. H. Dacol, F. Holtzberg, and D. K. Kaiser, Solid State Commun. **66**, 217 (1988).

[12]I. Poberaj, D. Mihailović, and S. Bernik (unpublished).